Accepted Manuscript

Original article

Iron pincer complex and its graphene oxide composite as catalysts for Suzuki coupling reaction

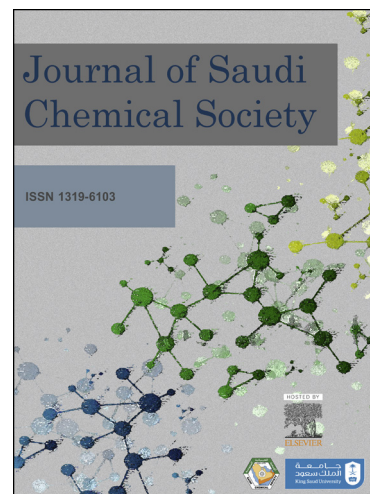Lolakshi Mahesh Kumar, Praveen Mishra, Badekai Ramachandra Bhat

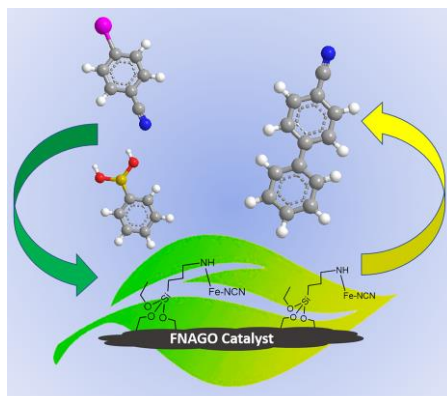## Graphical Abstract

To create your abstract, type over the instructions in the template box below.
Fonts or abstract dimensions should not be changed or altered.

Iron pincer complex and its graphene oxide composite as catalysts for Suzuki coupling reaction

Leave this area blank for abstract info.

Lolakshi Mahesh Kumar, Praveen Mishra, and Badekai Ramachandra Bhat*

Iron pincer complex and its graphene oxide composite as catalysts for Suzuki coupling reaction

Lolakshi Mahesh Kumar, Praveen Mishra, and Badekai Ramachandra Bhat*

Catalysis and Materials Laboratory, Department of Chemistry, National Institute of Technology Karnataka, Surathkal, Srinivasanagar-575025, India
* Corresponding Author: ram@nitk.edu.in

ARTICLE INFO

ABSTRACT

We report the synthesis of Fe-NCN pincer complex as homogenous catalyst and its composite by immobilizing the complex on amino functionalized graphene oxide as a heterogeneous catalyst for Suzuki coupling reactions. Both the complex and the composite were employed in catalyzing the Suzuki-Miyaura cross-coupling reaction between the aryl halide and phenyl boronic acid in acetonitrile solvent media with Cs_2CO_3 as a base. Effect of substitution over aryl halide was also investigated. Immobilization of the pincer complex had advantageous recovery and reuse of the catalyst as compared to its homogenous analogue with no significant decrease in the catalytic efficiency.

1. Introduction

In the late 1970s, the introduction of NCN diamine pincer ligand $[2,6-(Me_2NCH_2)_2-C_6H_3]-$ and its metal complexes by van Koten and group created a revolutionary progress in the field of pincer catalysis[1, 2]. The ligand has since then been extensively employed with different transition metals, predominantly with palladium to form complexes for wide range applications as catalysts in carbon-carbon bonding reactions[3-8], transfer hydrogenation reactions[9], silylcyanation of aldehydes[10], as gas sensing elements[11, 12], chemical switches[12], Friedel-Crafts alkylation[13], polymerization of dienes[14] and so on. The extensive application of the pincer motifs in several areas of chemistry follows their flexibility in modifying and fine-tuning of their properties[15]. The palladium-catalyzed coupling of an aryl halide with an organoboron compound, the Suzuki reaction, is regarded as one of the most efficient ways of forming a carbon-carbon bond[16]. However, relative less abundance of palladium on earth contributes to the high cost of the catalyst and the heaviness of the metal poses a hitch in its retrieval leading to toxicity. First-row transition metals could be alternatively used in the coupling reactions considering their characteristic catalytic potential combined with their low cost and low toxicity[17-19]. But the recovery of the catalyst and therefore need for extensive purification makes a homogenous reaction less appealing than its heterogeneous counterpart. Immobilization of the homogenous catalyst on an insoluble substrate can solve the recovery issue to a great extent, but the selection of the solid substrate plays a crucial role. There are numerous reports where catalyst have been immobilized on solid substrates like agar[20], cellulose[21], chitosan[22], starch[23], and other bio-compatible materials[24] for Suzuki coupling reactions. Graphene and its derivatives have been widely studied as a support to immobilize the catalysts due to their high strength and flexibility as solid substrates. They exhibit a very high surface area as compared to most of the available substrate which makes them a viable candidate to be used as a support for catalyst[25]. They have been used for supporting Pt nanoparticles for electro-oxidation of methanol[26]. Graphene oxide has also been looked up as a catalytic support for various direct organic reactions like oxidation and hydration[27] and few others[28]. Our attempts at synthesizing a suitable alternate to the expensive palladium catalysts worked out in the form of an iron pincer complex with a NCN ligand to act as a homogeneous catalyst. Further, we tried immobilizing this complex onto the graphene oxide substrate post functionalizing it with the amino group. Both the complex and composite were studied for their C-C coupling efficiency in the Suzuki-Miyaura coupling reaction.

2. Experimental

2.1. Materials

Iron (II) chloride, graphite powder (320 mesh, 99.5%), potassium permanganate ($KMnO_4$), conc. sulfuric acid (H_2SO_4), conc. hydrochloric acid, conc. nitric acid, phosphoric acid, hydrogen peroxide (H_2O_2 30%), 3-aminopropyltriethoxysilane (3-APTES) were purchased from Merck, India and used as received. 2-amino-4-nitrophenol, benzene-1,3-dicarboxaldehyde, phenylboronic acid and aryl halides were purchased from Sigma-Aldrich and tetrahydrofuran (THF), triethylamine (Et_3N), acetonitrile (ACN) were purchased from Alfa-Aesar and used without further purification.
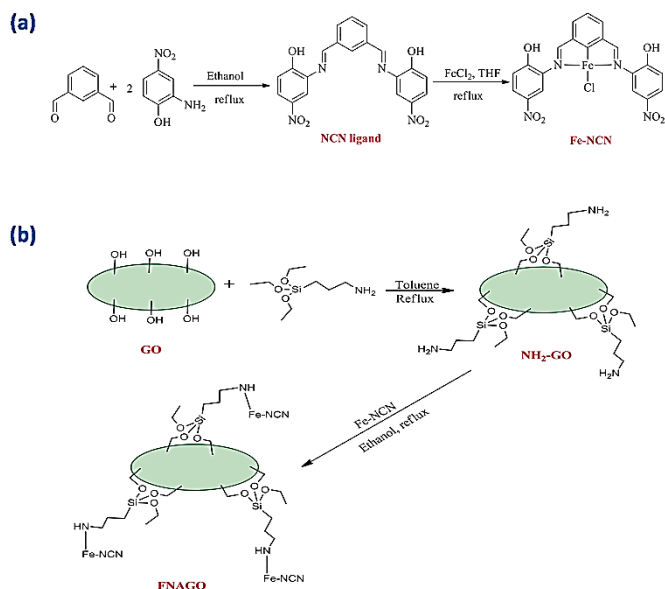
2.2. Synthesis of NCN ligand (NCN)

In a typical synthesis process, 0.2g of benzene-1,3-dicarboxaldehyde was stirred in ethanol (10 mL). 0.48g of 2-

amino-4-nitrophenol was added and the mixture was refluxed to obtain the Schiff base ligand (NCN). The solution was then filtered, washed with anhydrous hexane (2 x 10 mL) and the yellow solid was isolated (Scheme 1(a)).
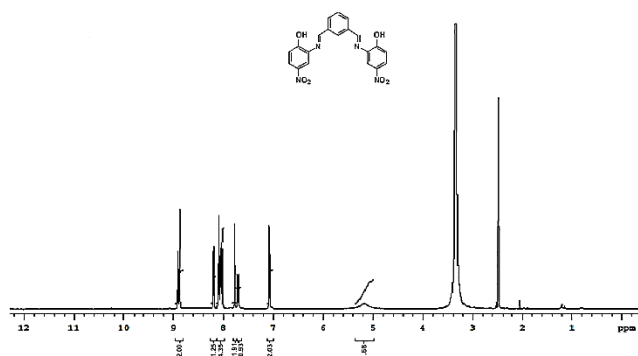
Yield: 91 %; ^{1}H NMR (400 MHz, CDCl$_3$) δ 8.82 (s, 2H), 8.24 (s, 1H) 8.17 – 8.05 (m, 4H), 7.78 (s, 2H), 7.76-7.67 (m, 1H), 7.08 (m, 2H), 5.18 (br s, 2H, OH) (Figure 1)
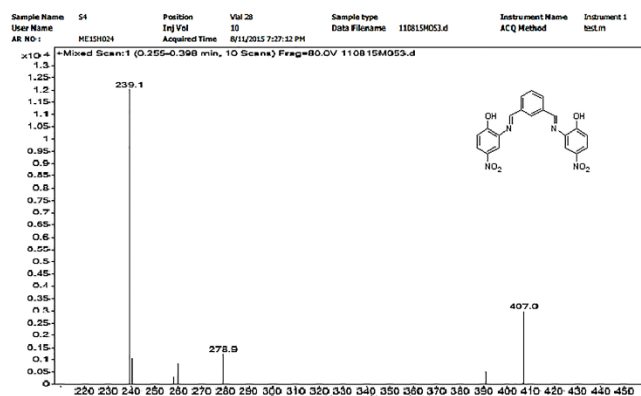
MS-ESI: (m/z): 407.0 (Figure 2)

Elemental analysis calculated for C$_{20}$H$_{14}$N$_4$O$_6$ (Mr = 406.1) (%): C, 59.12; H, 3.47; N, 13.79. Found: C, 58.90; H, 3.41; N, 13.81.

(a)

(b)

Scheme 1. (a) Synthesis of Fe-NCN complex; (b) Synthesis of Fe-NCN immobilized amino functionalized graphene oxide (FNAGO)

Figure 1. ^{1}H NMR spectrum of NCN ligand


Figure 2. ESI-Mass spectrum of NCN ligand

2.3. Synthesis of NCN complex

The prepared ligand (0.5 mmol) was taken in dry THF and refluxed with 0.5 mmol of iron chloride for 8 h. The precipitate obtained was decanted and washed with dry ether followed by filtration and drying at 50 °C in a vacuum oven for 4 h to obtain the iron pincer complex Fe-NCN (Scheme 1(a)).

Yield: 81%.

MS-ESI: (m/z): 496.2 [M]+ (Figure 3)

Elemental analysis calculated for C$_{20}$H$_{13}$ClFeN$_4$O$_6$ (Mr = 495.99) (%): C, 48.37; H, 2.64; N, 11.28. Found: C, 48.38; H, 2.55; N, 11.11.
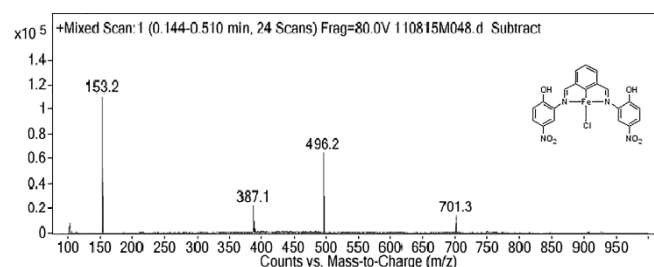
Figure 3. ESI-Mass spectrum of complex, Fe-NCN

2.4. Synthesis of Fe-NCN pincer complex on amino-functionalized graphene oxide (FNAGO)

Graphene oxide was prepared and purified using improved Hummers' method[29]. Graphene oxide substrate was functionalized with 3-aminopropyltriethoxysilane (3-APTES) as per the procedure reported elsewhere[30]. The resulting coated graphene oxide was dried in a vacuum oven at 40 °C for 24 h and labeled as amino-functionalized graphene oxide (NH$_2$–GO) (Scheme 1(b)). 1 g of this NH$_2$–GO was again dispersed in 30 mL ethanol and then 100 mg of Fe-NCN complex was added to prepare the iron composite (10%). The mixture was refluxed at 70 °C for 3 h. After cooling to room temperature, the mixture was filtrated and washed with ethanol to remove the undigested material, followed by drying. The resulting solid powder was labeled as FNAGO composite (Scheme 1(b)).

2.5. General procedure for the Suzuki reaction

To the mixture of phenylboronic acid (1.3 mmol) and Cs$_2$CO$_3$ taken in ACN (5 mL), synthesized pre-catalyst was added and allowed to stir for 30 min. Aryl halide (1.0 mmol) was then added slowly and the mixture refluxed until the reaction completes. The reaction mixture was monitored by Thin layer chromatography and Gas chromatography. The completed reaction was cooled to room temperature and the organic phase was decanted and washed with 1.5 N HCl and brine solution followed by drying with sodium sulphate and concentrated to obtain a crude product. The crude obtained was purified using column chromatography.

2.6. Characterization methods

The C, H and N contents of the compounds were determined by Thermoflash EA1112 series elemental analyzer. Magnetic susceptibility measurement was recorded on a Sherwood Scientific magnetic susceptibility balance (UK). FT-IR spectra were recorded on a Bruker-Alpha ECO-ATR FTIR spectrometer. ^{1}H NMR (400 MHz) spectrum was recorded in Bruker AV 400 instrument using TMS as an internal standard. The molecular mass of the compounds was determined using a Waters Q-Tof micro mass spectrometer with an ESI source. TGA was performed on Hitachi DTA-6300 with the heating rate of 10 ºC/min with minimum and maximum temperature being 29 ºC and 750 ºC,

respectively. 10% FNAGO was used for compositional and morphological studies. FNAGO was characterized by X-ray diffraction using Bruker AXS diffractometer D8 powder XRD to analyze its composition. The diffraction patterns were recorded at room temperature using a CuKα radiation (λ = 1.5418 Å) at a scan rate of 2 degree/min. Further, the compositional analysis was supported by using XPS analysis, which was recorded on Oxford Instruments-Omicron Nanotechnology XPS system (ESCA+) with a monochromatic Al-Kα radiation source of 1486.7 eV and 124 mm hemispherical electron analyzer. The morphology of FNAGO was analyzed using a Joel JSM-6380LA Scanning Electron Microscope. The samples were coated with gold using a sputter coating unit, to avoid charging during the recording. The coupling reaction product analysis was carried out using Gas Chromatography (GC) (Shimadzu 2014, Japan), siloxane Restek capillary column (30 m length and 0.25 mm diameter) and Flame Ionization Detector. The column temperature was increased at the rate of 10 °C/min with dinitrogen as the carrier gas.

3. Results and discussion

3.1. Characterization studies

The reaction of benzene-1,3-dicarboxaldehyde with 2-amino-4-nitrophenol resulted in the precipitation of Schiff base ligand (NCN) as a yellow solid in 91% yield. Formation of the imine ligand was confirmed by the singlet imine proton peak resonating at 8.82 ppm in ^{1}H NMR spectrum and further with the ESI-MS showing molecular weight peak at 407. FTIR spectrum (Figure 4(a)) shows the formation of the complex, Fe-NCN. Broad, strong O-H vibrational stretching peaks are observed in the frequency range of 3300-3400 cm^{-1} for both ligand and the complex and a medium absorption at 1686 cm^{-1} in the ligand spectrum corresponding to the C=N imine stretching shows a red shift in the spectra of the complexes[31]. Figure 4(b) depicts the transition from graphene oxide to FNAGO composite. In the FTIR spectrum of graphene oxide, peaks at 3370 cm^{-1}, 1630 cm^{-1} corresponds to the presence of O-H stretching and -C=O stretching. Also, C-OH stretching and C-O-C asymmetric stretching is reflected at 1170 cm^{-1} which cause broadening of the peak and the C-O-C symmetric stretching peak is observed at 1050 cm^{-1} respectively. In NH$_2$-GO spectrum, peaks corresponding to GO are present with a noticeable change in the peak at 3450 cm^{-1} due to the presence of N-H stretching indicating successful binding of APTES over GO and another peak at 620 cm^{-1} attributed to O-Si stretching. In FTIR spectra of FNAGO, the peaks corresponding to NH$_2$-GO are present with the addition to corresponding metal's fingerprint pattern. This suggests the formation of immobilized iron pincer ligand complex on the amino-functionalized GO.
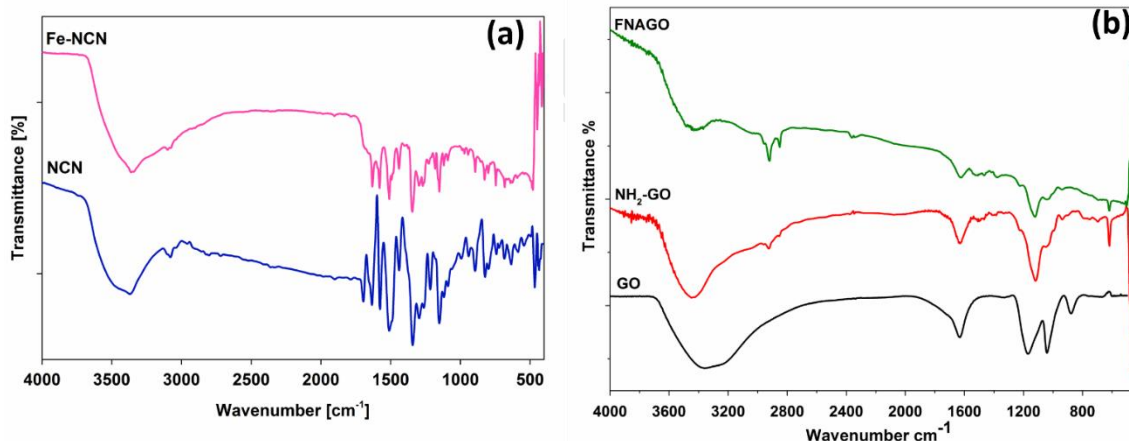
Figure 4. FTIR spectrum of (a) NCN ligand and Fe-NCN complex, and (b) Graphene oxide (GO), amino-functionalized GO (NH2-GO), and Fe-NCN immobilized amino functionalized GO (FNAGO).
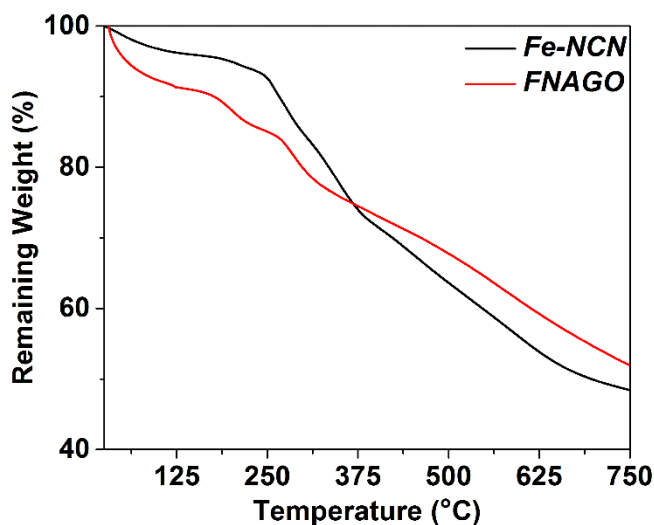
Figure 5. TGA of Fe-NCN and FNAGO

Room temperature magnetic moment value of 5.31 BM for Fe-NCN plainly suggests the iron metal with +2 oxidation state. Magnetic moment value indicates the presence of 4 unpaired electrons in the complex against the expected magnetic moment of 5.0 to 5.2 BM for Fe(II) four coordinated tetrahedral geometry[32].

The thermogravimetric analysis of the Fe-NCN complex and FNAGO composite presents the thermal stability of both the catalysts (Figure 5). The Fe-NCN complex showed better stability till 250 C, however, after this temperature, the decomposition of the complex is rapid. FNAGO has more gradual decomposition pattern which is due to the fact that GO, which is the substrate also undergoes thermal reduction along with the active complex. However, the low weight fraction of the complex w.r.t the substrate is the reason why the composite holds better thermal integrity at a higher temperature.

Figure 6 shows light on the surface morphology of the synthesized immobilized complexes on GO. APTES grafting over GO had very good surface coverage as evident for SEM of NH$_2$-GO. SEM image of FNAGO shows good coverage of Fe-NCN but, there is lack of well-defined shape of the covering, thereby rendering a more amorphous coating which is even evident from the XRD of the composite in Figure 7(a). The diffraction peak at 2θ equal to 11° corresponds to 001 plane of graphene oxide whereas at 26° is indicative of residual graphite in the sample. The intensity of these diffractions is observed to reduce in the composite XRD due to immobilization of the Fe-NCN complex

over NH₂-GO. The presence of the peak around 25º is due to reduced graphene oxide[33]. During NH₂-functionalization of GO, some GO gets reduced. Additionally, some graphitic particles also exist in GO which comes from the precursor. These leads to the characteristic graphitic peak at 2 theta value of 25º.

The composite surface was further studied through XPS analysis (Figure 7(b)). The XPS produced peaks corresponding to

C, Si-O and the iron metal which indicates the successful immobilization of the Fe-NCN complex on to the graphene oxide substrate. The carbon peak is observed at 285.4, a Si-O peak at 531.6 and the metal peak is seen at 708.1 corresponding to Fe.
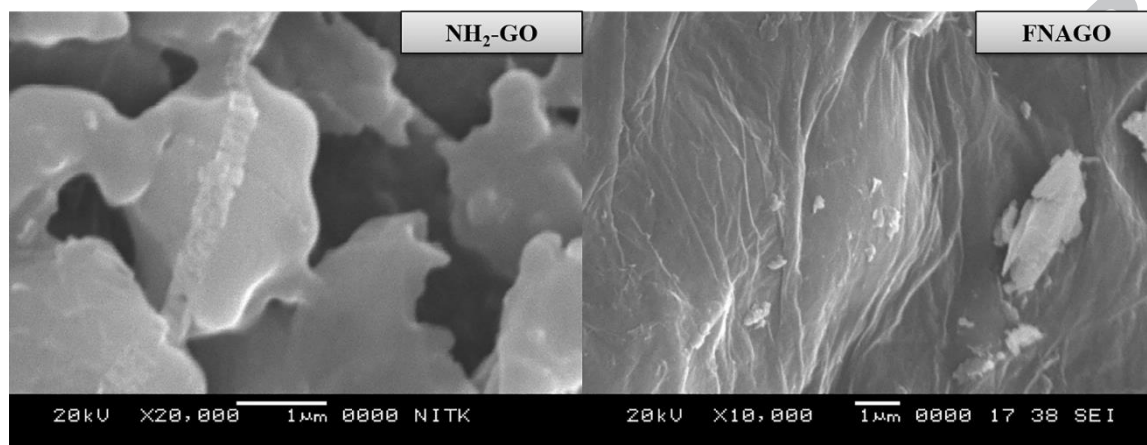

Figure 6. SEM of amino-functionalized graphene oxide (NH2-GO) and Fe-NCN immobilized amino functionalized GO (FNAGO)
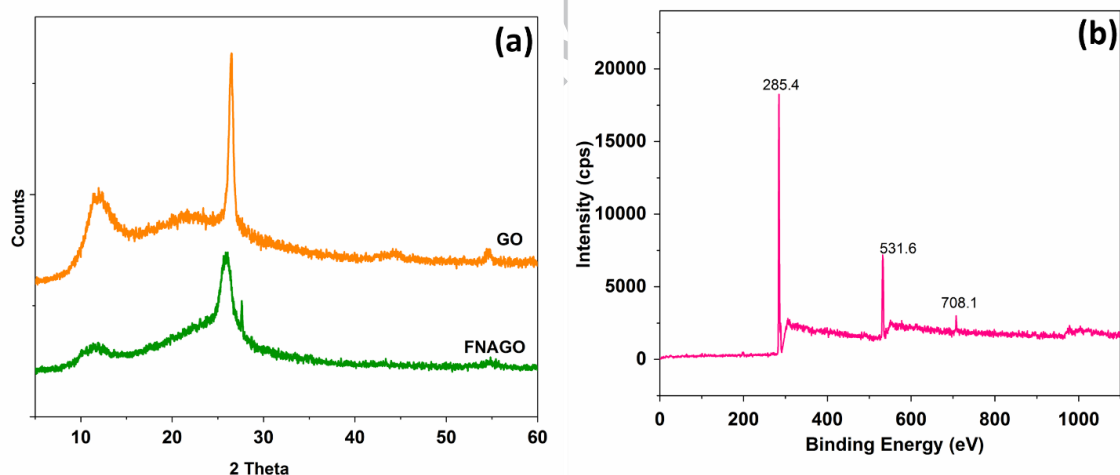

Figure 7. (a) XRD of graphene oxide (GO) and FNAGO; (b) XPS of FNAGO

3.2. Catalytic activity studies

Suzuki coupling reaction was chosen to examine the catalytic efficiency of the prepared complex and the composite. The reaction study included the reaction between aryl halides and phenylboronic acid in presence of acetonitrile[34] as a solvent, Cs_2CO_3[35] as a base and the Fe-NCN complex and its graphene oxide composite FNAGO as catalysts. Reaction parameters like catalyst loading and reaction time were screened to achieve high catalytic efficiency and yield. The reaction between 4-bromobenzonitrile and phenylboronic acid was chosen as a model reaction to evaluate the optimized catalytic activity.
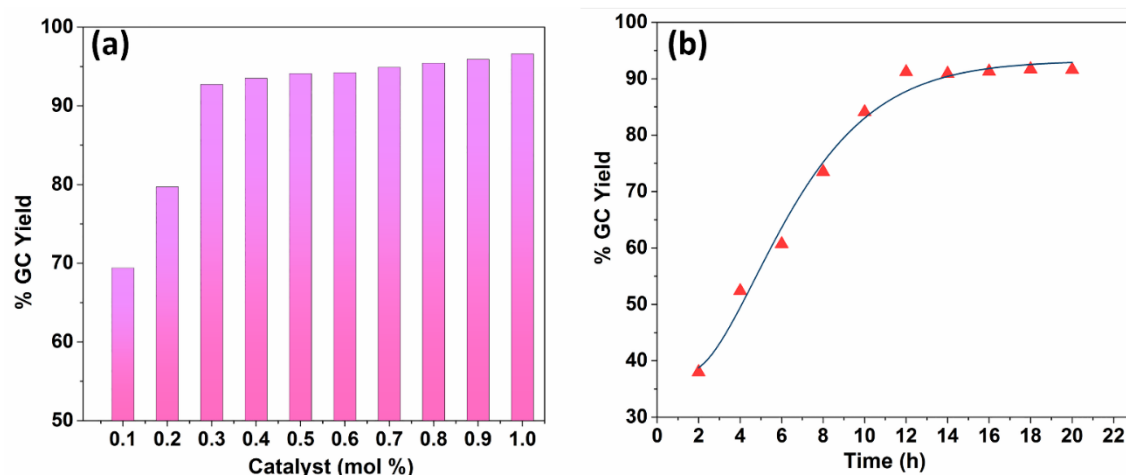
Influence of catalyst loading on the reaction efficiency was studied with different amount of the catalyst. Figure 8(a) shows the yield percentage vs. catalyst load with Fe-NCN loading varied from 0.1 mol % to 1.0 mol %. It is evident from the figure that the coupling efficiency is directly proportional to the catalyst input to a certain stage, further to which there is no obvious change in the catalytic yield. 0.3 mol% of the Fe-NCN was the optimized catalyst load concluded from the graph. The optimal time for coupling reaction was investigated by analyzing the reaction aliquots at regular intervals of time using the Fe-NCN as the

catalyst. A linear increase in the percentage yield could be observed for a period of 12 h of the reaction time for the pre-catalyst used (Figure 8(b)). An almost steady state in the yield could be observed for further 8 h, so optimized reaction time for the reactivity of the catalyst was considered as 12 h.

In case of FNAGO composite, different composites were prepared with the Fe-NCN complex loading varied from 5 % to 25 % based on the NH₂-GO weight. Figure 9(a) shows the yield percentage vs. catalyst load and the graph pattern concludes at 20 % FNAGO composite being the optimized catalyst load. The coupling reactions between substituted aromatic halides and phenylboronic acid were carried out with the optimized conditions and the results are summarized in Table 1.

The results highlight the coupling efficiency of aryl halides with electron withdrawing substituents in comparison to the electron donating groups. The FNAGO was also studied for its reusability in the reaction of 4-bromobenzonitrile with phenylboronic acid for 5 successive trials (Figure 9(b)). The catalytic conversion for all the trials was good with no significant reduction in the % GC yield indicating very good recovery and

reusability of the composite and showing advantage over the homogenous counterpart.

Figure 8. (a) Effect of catalyst loading on the yield of coupling reaction for homogenous catalysis using Fe-NCN catalyst; (b) Optimization of Reaction time using Fe-NCN catalyst for C-C- coupling reaction.
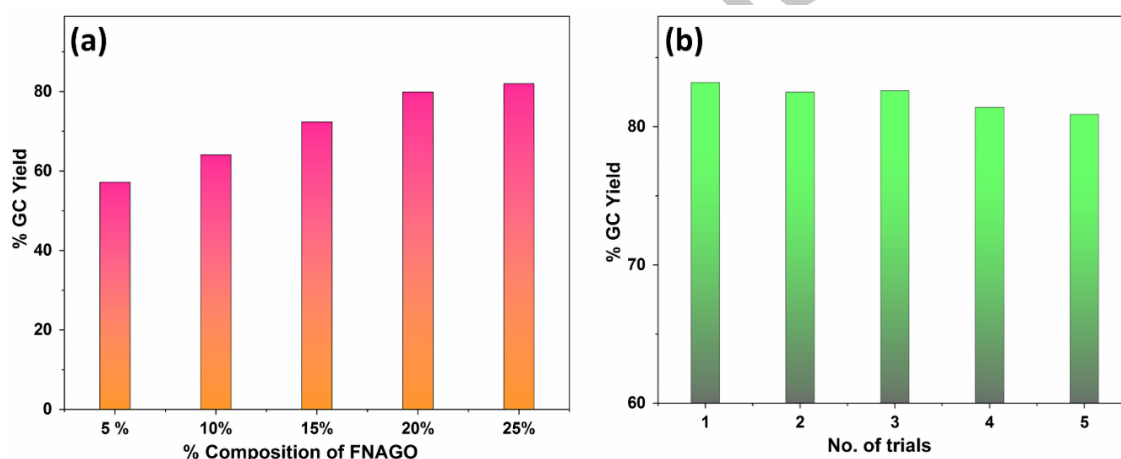
Figure 9. (a) Effect of % composition of FNAGO on the coupling yield for Heterogeneous catalysis; (b) Evaluation of reusability of FNAGO heterogeneous catalyst on the C-C coupling reaction

Table 1. Catalytic activity for Fe-NCN and FNAGO for C-C coupling between various aryl halide and phenyl boronic acids.

Entry	X	R	Yield (%)[a]	
			Fe-NCN	FNAGO
1	Br	CN	93 (89.4)	83
2		OCH$_3$	84	75
3		COCH$_3$	89 (83.8)	76
4		NHCOCH$_3$	93 (88.3)	84
5	I	OH	79	69
6		CN	98 (93.9)	89
7	Cl	CHO	79	68
8	Br	CN	Yield without using catalyst: Product not obtained	

Reaction conditions: Aryl halide (1.0 mmol), Phenylboronic acid (1.3 mmol), Cs$_2$CO$_3$ (2.0 mmol), catalyst: Fe-NCN - 0.3 mol%, FNAGO – 0.1 mmol (20 wt. % composite), ACN (5.0 mL), 12 h.
[a] GC yields, average of 3 trials (Isolated yield).

Figure 10 compares the surface morphology and IR spectra of FNAGO before and after the catalytic reaction. The surface of the FNAGO showed more deposits after the catalytic reactions which may be possibly due to the adsorption of the unspent reactants. The IR spectrum confirms this by the presence of aromatic CH stretching at 2500 cm^{-1} and broadening of the peaks at carbonyl region (1600-1800 cm^{-1}) which is due to the presence of carboxylic C=O in addition to the carbonyl groups presents on GO. Other peaks in the IR remained unchanged which indicates that the composite remains useful after the recovery from the reaction medium. The consistent activity after the reuse of the FNAGO composite as catalyst supports this observation (Figure 9b).
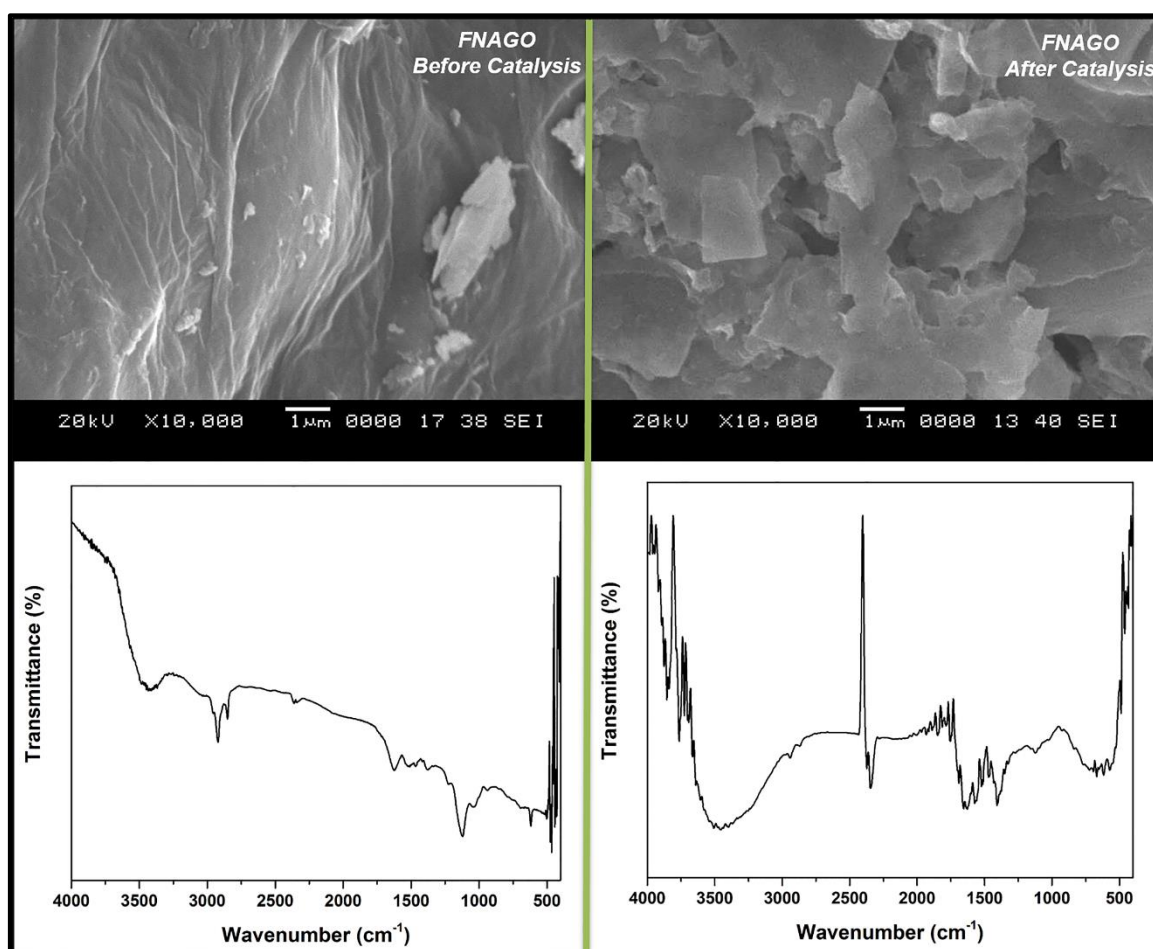
Figure 10. SEM and IR spectra of FNAGO composite before and after its use as a catalyst in the C-C coupling of aryl halides and phenyl boronic acid

4. Conclusions

NCN pincer complex with Fe metal was synthesized as an attempt to make available a complementary catalyst for the Suzuki-Miyaura coupling reaction. The main disadvantage of homogeneous catalysis i.e. recovery of the catalyst was overcome by the immobilization of the Fe-NCN pincer complex on graphene oxide. Fe-NCN and FNAGO efficiently catalyzed the coupling reaction between phenylboronic acid and aryl halides. The study also provided a direct comparison of a homogeneous and heterogeneous catalysis. The GC yield obtained for heterogeneous catalyst was approximately 10% lower than its homogenous counterpart; however, the catalyst can be reused multiple times with no much reduction in yield which is a significant advantage. The study construes the feasibility of iron as a catalytically active metal to efficiently substitute the Pd catalyzed reactions. Effortless synthesis of the catalysts, low cost of the starting materials used, and the efficient coupling conversion achieved, make the synthesized catalysts beneficial and viable in their catalytic approach.

Acknowledgments

References and notes

1   Ma, L.; Wobser, S. D.; Protasiewicz, J. D. *Journal of Organometallic Chemistry* **2007**, *692*, 5331.
2   van Koten, G.; Jastrzebski, J. T. B. H.; Noltes, J. G.; Spek, A. L.; Schoone, J. C. *Journal of Organometallic Chemistry* **1978**, *148*, 233.
3   Soro, B.; Stoccoro, S.; Minghetti, G.; Zucca, A.; Cinellu, M. A.; Manassero, M.; Gladiali, S. *Inorganica Chimica Acta* **2006**, *359*, 1879.
4   Fossey, J. S.; Russell, M. L.; Abdul Malik, K. M.; Richards, C. J. *Journal of Organometallic Chemistry* **2007**, *692*, 4843.
5   Slagt, M. Q.; Zwieten, D. A. P. v.; Moerkerk, A. J. C. M.; Gebbink, R. J. M. K.; Koten, G. v. *Coordination Chemistry Reviews* **2004**, *248*, 2275.
6   Gu, S.; Chen, W. *Organometallics* **2009**, *28*, 909.
7   Jung, I. G.; Son, S. U.; Park, K. H.; Chung, K.-C.; Lee, J. W.; Chung, Y. K. *Organometallics* **2003**, *22*, 4715.
8   Luo, Q.; Eibauer, S.; Reiser, O. *Journal of Molecular Catalysis A: Chemical* **2007**, *268*, 65.
9   Koten, G. v.; Dani, P.; Karlen, T.; Gossage, R.; Gladiali, S. *Angewandte Chemie* **2000**, *39*, 743.
10 Fossey, J. S.; Richards, C. J. *Tetrahedron Letters* **2003**, *44*, 8773.
11 Albrecht, M.; Gossage, R. A.; Frey, U.; Ehlers, A. W.; Baerends, E. J.; Merbach, A. E.; van Koten, G. *Inorganic Chemistry* **2001**, *40*, 850.
12 Albrecht, M.; van Koten, G. *Angewandte Chemie International Edition* **2001**, *40*, 3750.
13 Wu, L.-Y.; Hao, X.-Q.; Xu, Y.-X.; Jia, M.-Q.; Wang, Y.-N.; Gong, J.-F.; Song, M.-P. *Organometallics* **2009**, *28*, 3369.

14 Gao, W.; Cui, D. *Journal of the American Chemical Society* **2008**, *130*, 4984.

15 Morales-Morales, D. *Revista de la Sociedad Química de México* **2004**, *48*, 338.

16 Suzuki, A. *Angewandte chemie international edition* **2011**, *50*, 6722.

17 Bullock, R. M. *Catalysis without precious metals*; John Wiley & Sons, 2011.

18 Kulkarni, A. A.; Daugulis, O. *Synthesis* **2009**, *2009*, 4087.

19 Chakraborty, S.; Guan, H. *Dalton Transactions* **2010**, *39*, 7427.

20 Baran, T. *Carbohydrate Polymers* **2018**, *195*, 45.

21 Baran, T.; Yılmaz Baran, N.; Menteş, A. *Journal of Molecular Structure* **2018**, *1160*, 154.

22 Baran, T.; Açıksöz, E.; Menteş, A. *Journal of Molecular Catalysis A: Chemical* **2015**, *407*, 47.

23 Baran, T. *Journal of Colloid and Interface Science* **2017**, *496*, 446.

24 Baran, T.; Sargin, I.; Kaya, M.; Menteş, A. *Journal of Molecular Catalysis A: Chemical* **2016**, *420*, 216.

25 Yanwu, Z.; Shanthi, M.; Weiwei, C.; Xuesong, L.; Won, S. J.; R., P. J.; S., R. R. *Advanced Materials* **2010**, *22*, 3906.

26 Li, Y.; Gao, W.; Ci, L.; Wang, C.; Ajayan, P. M. *Carbon* **2010**, *48*, 1124.

27 R., D. D.; Hong-Peng, J.; W., B. C. *Angewandte Chemie* **2010**, *122*, 6965.

28 Jeffrey, P. *Angewandte Chemie International Edition* **2011**, *50*, 46.

29 Marcano, D. C.; Kosynkin, D. V.; Berlin, J. M.; Sinitskii, A.; Sun, Z.; Slesarev, A.; Alemany, L. B.; Lu, W.; Tour, J. M. *ACS Nano* **2010**, *4*, 4806.

30 Su, H.; Li, Z.; Huo, Q.; Guan, J.; Kan, Q. *RSC Advances* **2014**, *4*, 9990.

31 Sreekanth, A.; Prathapachandra Kurup, M. R. *Polyhedron* **2003**, *22*, 3321.

32 Barefield, E. K.; Busch, D. H.; Nelson, S. M. *Quarterly Reviews, Chemical Society* **1968**, *22*, 457.

33 Khan, M.; Al-Marri, A. H.; Khan, M.; Mohri, N.; Adil, S. F.; Al-Warthan, A.; Siddiqui, M. R. H.; Alkhathlan, H. Z.; Berger, R.; Tremel, W.; Tahir, M. N. *RSC Advances* **2014**, *4*, 24119.

34 Dyson, P. J.; Jessop, P. G. *Catalysis Science & Technology* **2016**, *6*, 3302.

35 Rabie, R.; Hammouda, M. M.; Elattar, K. M. *Research on Chemical Intermediates* **2017**, *43*, 1979.